горения, $\varkappa$ — температуропроводность состава. Для реальных композиций с полидисперсным окислителем и активной связкой картина влияния дисперсности компонентов на нестационарные характеристики горения более сложна. Требуются дополнительные экспериментальные исследования подобных систем для выявления влияния дисперсности и компонентного состава топлива на нестационарные характеристики горения.

ЛИТЕРАТУРА

1. **Илюхин В. С., Марголин А. Д., Сверчков Ю. Е.** Исследование переходных процессов горения крупнозернистых смесевых топлив // Горение конденсированных систем.— Черноголовка, 1977.
2. **Илюхин В. С., Марголин А. Д., Валеев И. И. и др.** Влияние размера частиц окислителя на время нестационарного горения смесевого твердого топлива при сбросе давления // ФГВ.— 1987.— 23, № 3.
3. **Симоненко В. Н., Кискин А. Б., Фоменко В. М. и др.** Исследование отклика скорости горения порохов на периодическое воздействие лазерного излучения // Горение конденсированных систем.— Черноголовка, 1986.

г. Новосибирск

УДК 536.46

T. Dagusé, A. Soufiani, N. Darabiha, J. C. Rolon

STRUCTURE OF DIFFUSION AND PREMIXED LAMINAR COUNTERFLOW FLAMES INCLUDING MOLECULAR RADIATIVE TRANSFER

Laboratoire d'Energétique Moléculaire et Macroscopique, Combustion du CNRS et de l'ECP, Ecole Centrale Paris
Grande Voie des Vignes, 92295 Chatenay-Malabry, France

Abstract

The interaction between radiation and combustion is studied theoretically in the case of strained counterflow nonluminous laminar flames. Both $H_2 - O_2$ diffusion and C_3H_8 — air premixed flames are considered. Calculations are based on detailed chemical kinetics and narrow-band statistical modeling of infrared radiative properties. It is shown that radiative transfer decreases the temperature level, which affects particularly the production and consumption of minor species and pollutants. For $H_2 - O_2$ flames, a low strain rate extinction limit due to radiation is found. It is also shown that the commonly used approximation of optically thin medium is inaccurate, even for the small scale laboratory flames considered here.

Introduction

It is well established that radiation is an important heat transfer mode in industrial large scale flames. For non-sooty, small scale laboratory flames, radiative losses represent generally a small fraction of the chemical heat release. Thus, radiation effects are the most often neglected in the studies related to flame modeling. However, radiative transfer leads to a decrease of flame temperature, which may induce large variations of some flame properties. Some of these temperature dependent properties are: (i) production of some minor species, in particular pollutants, (ii) flammability limits, and (iii) flame propagation velocity.

Liu et al. [1] have studied experimentally radiation effects on temperature profiles in double premixed CH_4 — air flames. Liu and Rogg [2] investigated the case of $CO/H_2/N_2$ — air diffusion flames and showed important effects of radiation on NO and NO_2 production. Lakshmisha et al. [3] and Sibulkin and Frendi [4] have studied the flammability limits and flame velocities, taking into account radiation, in lean premixed CH_4 — air flames.

They show that radiative transfer is an important mechanism, explaining the flame extinction in some lean propagating flames. T'ien [5] pointed out the importance of radiative transfer in the case of low strain rates. However, in all the above studies, radiative transfer has been modeled by using the simplified approach of optically thin media and the mean Planck absorption coefficient [1—4], or by considering the flame as a blackbody radiating medium [5]. Negrelli et al. [6] have discussed the accuracy of the model using the mean Planck absorption coefficient and optically thin approximation.

In this paper, we study theoretically radiation-combustion interactions in strained laminar, counterflow flames. The results presented here are related to typical $H_2 - O_2$ diffusion flames and C_3H_8 — air premixed flames. We use a detailed chemistry model and a statistical narrow-band representation of radiative properties, as described in section 2. In section 3 we present radiation effects on the flame structure and the evolution of this structure with the strain rate.

Problem formulation

The flame configuration considered in the present calculations is a counterflow, axisymmetrical laminar flame, stabilized near the stagnation plane of two opposed jet flows. The numerical prediction of these flames, considered as adiabatic, is now standard and widely described in the literature (see for instance [7—8] for diffusion flames and [9, 10] for premixed flames). In this study, we model the counterflow strained laminar flames by searching for similar solutions of the different variables with the classical boundary layer assumption. The governing equations along the symmetry axis are written in conservation form for mass, momentum and chemical species and are completed with the perfect gas state equation [7—10]. Only the energy balance equation is modified in order to take into account radiative transfer:

$$c_p V \frac{dT}{dy} - \frac{d}{dy}\left(\lambda \frac{dT}{dy}\right) + \left(\sum_{k=1}^{K} \rho Y_k V_{ky} c_{pk}\right) \frac{dT}{dy} + \sum_{k=1}^{K} h_k W_k \omega_k + S_R = 0,$$

where S_R is the radiative volumetric source term. The similar solutions have the form $\rho = \rho(y)$, $u = \varepsilon r U(y)$, $v = V(y)/\rho(y)$, $T = T(y)$ and $Y_k = Y_k(y)$, $k = 1, \ldots, K$, where y denotes the spatial coordinate normal to the stagnation plane, ρ, u, v, T and Y_k are respectively the density, velocity components, temperature and mass fraction of the k^{th} species. The constant ε designates the strain rate defined by $u(r, +\infty) = \varepsilon r$, U and V designate a reduced velocity and the normal mass flux, respectively. The conservation equations are completed by formula expressing the transport coefficients (λ, μ), the diffusion velocities (V_{ky}), the thermodynamic properties (c_p, c_{pk}, h_k) and the chemical production rates (ω_k) in terms of the state variables, T, p, Y_k and their gradients. These data, which involve detailed transport and complex chemical kinetics, are determined by using CHEMKIN and TRANSPORT packages [11, 12] in a vectorized form as explained in [13].

For non-luminous flames, the radiative source term S_R is due both to infrared vibration — rotation bands of products such as CO_2, H_2O and CO, and to visible and UV radiation resulting from electronic transitions of free radicals such as OH, CH and C_2. We have compared the amount of UV and IR radiation in the simple case of $H_2 - O_2$ flames where the main contribution to UV emission is due to the $A^2\Sigma \rightarrow X^2\Pi$ electronic transition of the radical OH, centered near 32.684 cm^{-1}. For the same flame, infrared radiation results mainly from the vibration-rotation bands of water vapor. A line-by-line procedure has been used to compute the high-resolution ultraviolet OH emission spectrum. The energy values are taken from [14] and the Einstein emission coefficients for the individual transitions from [15]. Emission lines were assumed to have a Voigt profile with mean

Lorentz half-widths taken from [16]. Under the assumption of thermodynamic equilibrium, the total ultraviolet intensity emitted by an isothermal and homogeneous column of length $l = 10$ cm, at $T = 2500$ K and $p = 1$ atm with a OH molar fraction $x_{OH} = 2.5 \cdot 10^{-2}$ is about $I_{UV} = 0.99 Wm^{-2}sr^{-1}$. For the same column with a water vapor molar fraction $x_{H_2O} = 0.34$, the emitted infrared intensity, computed from a statistical narrow-band model, is $I_{IR} = 7144\ Wm^{-2}sr^{-1}$. We may conclude that the OH ultraviolet radiation may be neglected in comparison with H_2O infrared emission if the Maxwell — Boltzmann distribution holds for OH energy levels. But a departure from this thermodynamic equilibrium may occur in some flames as discussed in [17]. In the following, we consider only radiative transfer in the infrared range.

For the flames considered in this study, the main radiating gases are H_2O in $H_2 - O_2$ flames and H_2O, CO_2 and CO in C_3H_8 — air flames. IR radiative properties of such molecules are modeled by using a statistical narrow-band model with the exponential tailed-inverse distribution of line intensities [18]. The transmissivity $\bar{\tau}_\nu$ of an isothermal and homogeneous column of length l, averaged over a spectral range $\Delta\nu$ is given by

$$\bar{\tau}_\nu = \exp\left[-\frac{\bar{\beta}}{\pi}\left(\sqrt{1 + \frac{2\pi x p l \bar{k}}{\bar{\beta}}} - 1\right)\right],$$

where x and p are the molar fraction of the absorbing species and the total pressure, respectively, $\bar{k}$ and $\bar{\beta}$ are the model parameters related to the spectroscopic properties of the absorption lines inside $\Delta\nu$ [19]. The statistical narrow-band model is used here with a low spectral resolution $\Delta\nu = 25\ cm^{-1}$ in the range 150—6000 cm^{-1}, including the most influent vibration-rotation bands for the temperature range considered here. The model parameters are deduced from line-by-line calculations as described in [19, 20]. The transmissivity of non-homogeneous and non-isothermal columns is computed by using the Curtis — Godson approximation which has been proved to be accurate for optical paths at constant pressure [19, 21].

The radiative transfer equation for an absorbing and emitting but non-scattering medium is written in terms of transmissivities

$$\bar{I}_\nu(s) = \bar{I}_\nu(0)\,\bar{\tau}_\nu(0, s) + \int_0^s I_\nu^b(s')\,\frac{\partial \bar{\tau}_\nu}{\partial s'}(s', s)\,ds',$$

where I_ν^b designates the equilibrium or blackbody intensity and $\bar{\tau}_\nu(s', s)$ the transmissivity of the heterogeneous column between the abscissae s' and s. The radiative source term in the energy conservation equation is obtained by integration of $\partial I_\nu / \partial s$ over the wave number ν and the propagation direction

$$S_R = \int_0^\infty \int_{4\pi sr} \frac{\partial \bar{I}_\nu}{\partial s}(s, \vec{u})\,d\Omega\,d\nu.$$

In radiative transfer computations, we use a planar infinite geometry consistent with the flow field model. For the radiative boundary conditions, we consider that the flame is inside an environment at room temperature. For this planar geometry, this is equivalent to assume that the flame is bounded by two infinite black parallel plates at room temperature. The radiative transfer equation, associated to these boundary conditions, is solved by using a pure numerical method described in detail in [19, 22]. It is worth noticing that this procedure does not use any approximation concerning the medium optical thickness.

The conservation equations associated to their boundary conditions are solved numerically by using a finite difference unsteady formulation [8]. If we except the radiative source term in the energy equation, a fully implicit scheme is used where the non-linear terms are linearized following a method

similar to that of Briley and McDonald [23]. The radiative field is calculated, at a given iteration step, from the previous temperature and molar fraction fields.

Results and Discussion

Two configurations of atmospheric flames have been considered in this study: the strained diffusion flame in the counterflow of oxydant ($O_2 + N_2$) and fuel ($H_2 + N_2$) and the strained premixed double flame in the counterflow of two identical fresh reactant mixtures (C_3H_8 — air). In both cases, the inlet gas temperatures are 300 K.

Calculations are based on the kinetics given by Westbrook and Dryer [24] which contains 123 elementary step reactions and 31 species for C_3H_8 — air flames. This scheme is completed by the NO_x formation mechanism as recommended by Miller and Bowman [25]. Calculations have been carried out for a large number of parameters such as the strain rate and inlet mass fractions of oxydant and fuel. Only typical results are shown in the following.

Radiative effects on flame structure are expected to be the most important when the rate of radiative loss becomes substantial in comparison with the rate of chemical heat release. The ratio between these energies depends in our computations on the strain rate and inlet mass fractions of different species. As a result of the competition between convection and molecular diffusion phenomena in the reaction zone, the flame thickness, maximum temperature and product mass fractions increase when the strain rate decreases. Additionally, when the strain rate decreases, the chemical production term in the energy equation decreases.

Figure 1 represents temperature and NO mass fraction profiles computed with and without radiation in the case of the H_2 — O_2 diffusion flame. Two relatively small values of the strain rate are considered on this figure ($\varepsilon = 0.1$ s^{-1} and $\varepsilon = 2$ s^{-1}). It is seen that radiation leads to a maximum temperature decrease of about 150 K for $\varepsilon = 2$ s^{-1} and 1080 K for $\varepsilon = 0.1$ s^{-1} (Fig. 1.*a*). In all cases, temperature and H_2O mole fraction profiles are wider than the chemical heat release pofiles. The ratio of radiation loss to chemical heat release is much higher at the edges of the flame front than at the flame centre. As a consequence, radiative transfer leads to a decrease of flame thickness. The effects of radiation on the concentration of major species are found to be small. On the other hand, radiative transfer is found to be an important mechanism in the thermal production of NO as shown in Fig. 1.*b*. Similar decrease of mass fraction are found for OH.

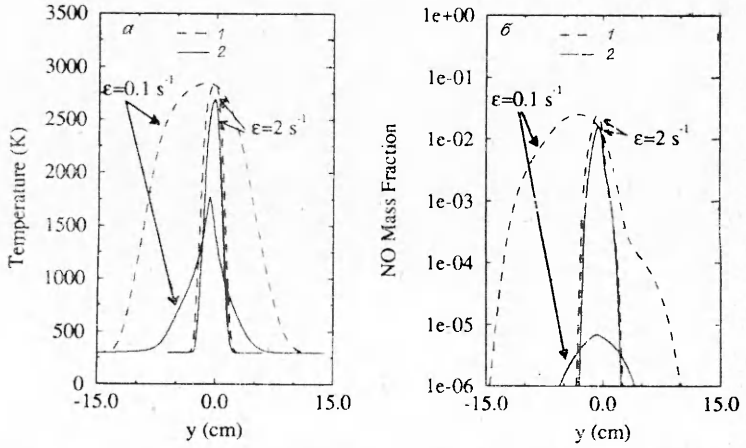

Fig. 1. Temperature and NO mass fraction profiles for a strain rate of 0.1 s^{-1} and 2 s^{-1}. The inlet mass fractions are $Y_{O_2} = 1$ and $Y_{H_2} = 0.1$.

1 — without Radiation; *2* — with Radiation.

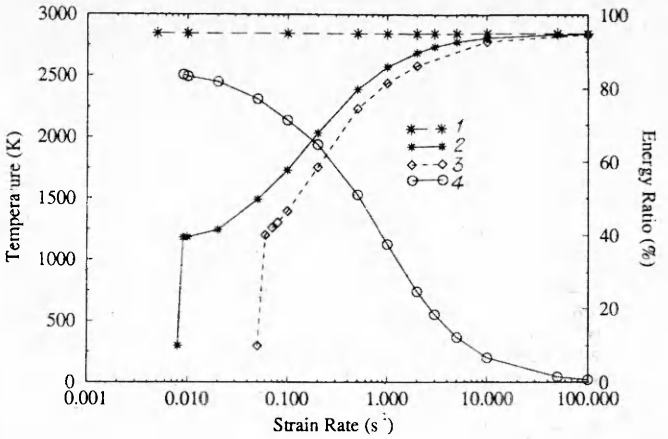

Fig. 2. Maximum temperature and integrated radiative loss and chemical heat release ratio R as a function of the strain rate. The inlet mass fractions are $Y_{O_2} = 1$ and $Y_{H_2} = 0.1$.

1 — T_{max} without radiation; 2 — T_{max} with the detailed rad. model; 3 — T_{max} with the O. T. M. approxim.; 4 — energy ratio.

In double premixed flames, the situation is slightly different since emission from the volume between the flame surfaces is greater than the emission from the flame fronts themselves. We have found a strong decrease of temperature between the flame fronts at low values of the strain rate and a decrease of the distance between the flame fronts as noticed by Sohrab and Law [26].

We have also studied the influence of radiation on the extinction limits of $H_2 - O_2$ diffusion flames. For the lean extinction limit, temperature and H_2O mole fraction decrease with the equivalence ratio in such a manner that radiative losses decrease faster that the chemical heat release. Thus, we found only very small effects of radiative transfer on the lean extinction limit.

For diffusion flames considered as adiabatic, a decrease in strain rate increases the flame thicknes and flame maximum temperature tends to a constant value. At the same time, the chemical heat release rate per unit volume decreases almost proportionally to the strain rate. Figure 2 gives the evolution of the maximum temperature as a function of the strain rate when radiative transfer is taken into account. This figure also gives the ratio between the integrated radiative loss and the chemical heat release rates:

$$R = \frac{\int_{-\infty}^{\infty} S_R dy}{\int_{-\infty}^{\infty} \left(\sum_{k=1}^{K} h_k \omega_k W_k \right) dy}.$$

This ratio reaches 80 % while the maximum temperature decreases from 2850 K to 1180 K due to radiative losses for $\varepsilon = 0.009$ s^{-1}. If we consider the flame structure at this value of the strain rate as an initial condition and look for the solution at $\varepsilon = 0.008$ s^{-1}, the temperature decreases rapidly during time iteration steps and reaches 300 K. This means that a low strain rate extinction limit for this flame is found for ε close to 0.008 s^{-1}, but such strain rates are not frequently encountered in practical applications.

We have also carried out some calculations by considering the flame as an optically thin medium (OTM) and by using the mean Planck absorption coefficient given by Hubbard and Tien [27]. It is shown on Fig. 2 that the use of this model leads to an overestimation of radiative losses. With this model, the extinction limit is obtained at $\varepsilon = 0.05$ s^{-1} which is six times greater than the value obtained when using the detailed radiative model.

Indeed, even for the small scale laboratory flames considered here, there are many intense absorption lines for which absorption cannot be neglected in the energy balance equation. If one considers the flame surface as a black-body radiator, as it is done by T'ien [5], extinction is found at higher values of the strain rate.

REFERENCES

1. **Liu G. E., Ye Z. Y., Sohrab S. H.** On radiative cooling and temperature profiles of counterflow premixed flames // Combust. Flame.— 1986.— **64.**— P. 193—201.
2. **Liu Y., Rogg B.** Modelling of thermally radiating diffusion flames with detailed chemistry and transport. Eurotherm Seminar N17 «Heat Transfer in Radiating and Combusting Systems», Cascais, Portugal, 1990.
3. **Lakshmisha K. N., Paul P. J., Mukunda H. S.** On the flammability limits and heat loss in flames with detailed chemistry // 23rd Symp. (Int.) on Combust., paper n 23—510, Orleans, France, 1990.
4. **Sibulkin M., Frendi A.** Prediction of flammability limit of an unconfined premixed gas in the absence of gravity // Combust. Flame.— 1990.— **82.**— P. 334—345.
5. **T'ien J. S.** Diffusion flame extinction at small stretch rates: the mechanism of radiative loss // Ibid.— 1986.— **65.**— P. 31—34.
6. **Negrelli D. E., Lloyd J. R., Novotny J. L.** A theoretical and experimental study of radiation-convection interaction in a diffusion flame // J. Heat Transfer.— 1977.— **99.**— P. 212—220.
7. **Smooke M. D., Puri I. K., Sehardi K.** A comparison between numerical calculations and experimental measurements of the structure of a counterflow diffusion flame burning diluted methane and diluted air // 21st Symp. (Int.) on Combust., Reinhold, N. Y., 1986.
8. **Darabiha N., Candel S.** The influence of the temperature on the extinction and ignition limits of strained hydrogen — air diffusion flames. In press in Combust. Sci. and Technol.
9. **Libby P. A., Linan A., Williams F. A.** Strained premixed laminar flames with nonunity Lewis number // Combust. Sci. and Technol.— 1983.— **34.**— P. 257—293.
10. **Giovangigli V., Smooke M. D.** Extinction of strained premixed laminar flames with complex chemistry // Ibid.— 1987.— **53.**— P. 23—49.
11. **Kee R. J., Miller J. A., Jefferson T. H.** CHEMKIN: a general-purpose, transportable, Fortran chemical kinetics code package // Sandia National Lab. Report, SAND80—8003.— 1980.
12. **Kee R. J., Warnatz J., Miller J. A.** A Fortran computer code package for the evaluation of gas-phase viscosities, conductivities, and diffusion coefficients // Sandia National Lab. Report, SAND83-8209.— 1983.
13. **Darabiha N., Giovangigli V.** Vectorized computation of complex chemistry flames // Proc. Int. Symp. on High Performance Computing, Elsevier Sci. Publ., Montpellier, France, 1989.— P. 273—285.
14. **Dieke G. H., Crosswhite H. M.** The ultraviolet bands of OH. Fundamental data // J. Quant. Spectrocs. Radiat. Transfer.— 1962.— **2.**— P. 97—199.
15. **Chidsey I. L., Crosley D. R.** Calculated rotational transition probabilities for the A — X system of OH // J. Quant. Spectrosc. Radiat. Transfer.— 1980.— **23.**— P. 187—199.
16. **Rea E. C., Chang A. Y., Hanson R. K.** Collisional broadening of the $A^2\Sigma^+ - X^2\Pi$ band of OH by H_2O and CO_2 in atmospheric-pressure flames // Ibid.— 1989.— **41.**— P. 29—42.
17. **Gaydon A. G., Wolfhard H. G.** Flames. Their structure, radiation and temperature. Forth ed. N. Y., John Wiley-Sons, 1979.
18. **Malkmus W.** Random Lorentz band model with exponential tailed S^{-1} line-intensity distribution // J. Opt. Soc. Am.— 1967.— **57.**— P. 323—329.
19. **Soufiani A., Hartmann J. M., Taine J.** Validity of band-model calculations for CO_2 and H_2O applied to radiative properties and conductive-radiative transfer // J. Quant. Spectrosc. Radiat. Transfer.— 1985.— **33.**— P. 243—257.
20. **Hartmann J. M., Levi Di Leon R., Taine J.** Line-by-line and narrow-band-statistical model calculations for H_2O // Ibid.— 1984.— **32.**— P. 119—127.
21. **Young S. J.** Nonisothermal band model theory // Ibid.— 1977.— **18.**— P. 1—28.
22. **Soufiani A., Taine J.** Application of statistical narrow-band model to coupled radiation and convection at high temperature // Int. J. Heat Mass Transfer.— 1987.— **30.**— P. 437—447.
23. **Briley W. R., McDonald H.** On the structure and use of linearized block implicit schemes // J. Comput. Phys.— 1980.— **34.**— P. 54—73.
24. **Westbrook C. K., Dryer F. L.** Chemical kinetic modeling of hydrocarbon combustion // Prog. Energy and Combust. Sci.— 1984.— **10.**— P. 1—57.
25. **Miller J. A., Bowman C. T.** Mechanism and modeling of nitrogen in combustion // Ibid.— 1989.— **15.**— P. 287—338.
26. **Sohrab S. H., Law C. K.** Extinction of premixed flames by stretch and radiative loss // Int. J. Heat Mass Transfer.— 1984.— **27.**— P. 291—300.
27. **Hubbard G. L., Tien C. L.** Infrared mean absorption coefficients of luminous flames and smoke // J. Heat Transfer.— 1978.— **100.**— P. 235—239.